Magnetic ground state of $CeNi_{1-x}Cu_x$: A calorimetric investigation

N. Marcano, J. I. Espeso, J. C. Gómez Sal, and J. Rodríguez Fernández
Departamento de Ciencias de la Tierra y Física de la Materia Condensada, Facultad de Ciencias, Universidad de Cantabria, 39005 Santander, Spain

J. Herrero-Albillos and F. Bartolomé
Instituto de Ciencia de Materiales de Aragón, CSIC Universidad de Zaragoza, 50009 Zaragoza, Spain
(Received 8 November 2004; published 6 April 2005)

$CeNi_{1-x}Cu_x$ is a substitutional magnetic system where the interplay of the different magnetic interactions leads to the disappearance of the long-range magnetic order on the CeNi side. The existence of inhomogeneities (spin clusters or phase coexistence) has been previously detected by magnetization and muon spin relaxation (μSR) spectroscopy measurements. These inhomogeneities are always observed regardless of the different preparation methods and must, then, be considered as intrinsic. We present a detailed specific heat study in a large temperature range of 0.2 to 300 K. The analysis of these data, considering also previous neutron scattering, magnetic characterization, and μSR results, allows us to present a convenient description of the system as inhomogeneous on the nanometric scale. Two regimes are detected in the compositional range depending on the dominant Ruderman-Kittel-Kasuya-Yosida or Kondo interactions. We propose that the long-range magnetic order at low temperatures is achieved by a percolative process of magnetic clusters that become static below the freezing temperature T_f. In this scenario the existence of a quantum critical point at the magnetic-nonmagnetic crossover must be discarded. This situation should be considered as an example for other substitutional compounds with anomalous magnetic or superconducting properties.

DOI: 10.1103/PhysRevB.71.134401 PACS number(s): 75.40.−s, 65.40.Ba, 75.30.Mb

I. INTRODUCTION

Strongly correlated electron metals have been for a long time now one of the most fruitful fields for the discovery of new physical phenomena (heavy fermions, non-Fermi liquids (NFL's), quantum critical points (QCP's), or unconventional superconductivity), some of them pointing toward a possible new description of the quasiparticle ground state. At the same time, the study of such magnetic compounds has provided additional insight into the understanding of the basic magnetic interactions (Ruderman-Kittel-Kasuya-Yosida RKKY, $4f$-$3d$ hybridization, crystal electric field, etc.) and the interplay between them.

In many of these systems an additional problem appears when we are dealing with atomic substitutions. This problem is described in general as "disorder effects" and could consist of compositional local inhomogeneities, phase coexistence, and clusterization processes that in most cases are intrinsic to the samples and cannot be avoided by means of different preparation methods or supplementary thermal treatments.

Specific heat (C_P) measurements provide a powerful method for studying the behavior of these compounds[1] for the following reasons.

(i) The magnetic contribution to the specific heat and the corresponding magnetic entropy are related to the energy levels of the magnetic ions (cerium in our case) and the shape of the anomalies corresponding to the magnetic phase transition gives a valuable indication as to the nature of the transition.

(ii) The electronic coefficient γ provides relevant information concerning the conduction band density of states at the Fermi level.

(iii) At higher temperatures the shape of the thermal variation of the specific heat depends on the crystal electric field splitting.

(iv) The very-low-temperature C_P/T behavior can show departures from the predictions of the Fermi-liquid theory,[2] which could serve as the sign of the different scenarios devoted to explaining the physics involved in these processes (spin fluctuations that exist close to a QCP,[3–5] Griffiths phase situation,[6] disorder-driven mechanisms like "Kondo disorder,"[7,8] etc.).

All these features can be used in the analysis of the $CeNi_{1-x}Cu_x$ system, which has been studied over the last few years with different macroscopic and microscopic techniques such as magnetization, resistivity, neutron diffraction, muon spin relaxation (μSR) spectroscopy, etc. The main features of this system at the present stage can be summarized as follows.

(a) A complex magnetic behavior was determined[9] with a change from an antiferromagnetic (AFM) (CeCu) to ferromagnetic (FM) ground state well characterized by neutron diffraction in $CeNi_{0.4}Cu_{0.6}$ (Ref. 10) evolving toward the evanescence of the long-range magnetic order around $CeNi_{0.8}Cu_{0.2}$.

(b) A "spin-glass-like" phase was surprisingly found at temperatures above the ferromagnetic order state.[11] A "cluster-glass" scenario seems the most plausible hypothesis according to ac and dc magnetization measurements.[12]

(c) In fact, recent μSR studies confirm the presence of a highly inhomogeneous magnetic state at temperatures extending from the long-range ordered ground state to the paramagnetic regime. This inhomogeneous magnetic state consists of long-range ordered and nonordered fractions, the latter increasing with temperature.[13]

(d) The Ni-rich part of the diagram is very sensitive to thermal treatments due to the proximity to the crystalline structural change (FeB to CrB).[14] There appears a marked decrease in magnetization as a consequence of the strong reduction of the magnetic Ce moments due to the increasing hybridization effects. Some traces of hysteresis, however, have been detected at very low temperatures in the $CeNi_{0.85}Cu_{0.15}$ and $CeNi_{0.9}Cu_{0.1}$ compounds, which show that the magnetic moments have not been completely exhausted yet.[15]

Many questions still await answers in order for there to be a full understanding of such complex behavior. The aim of this paper is to show how the specific heat measurements performed in these series between 0.2 and 300 K provide valuable information that sheds light on the underlying physics in the system.

Starting in the first part of the article with a detailed presentation of the preparation methods, crystallography, and quality control of the samples, we go on to present the specific heat measurements and their corresponding analysis. Special care has been taken in order to elucidate the nature of the anomalies found in these compounds. Particular attention has been paid to the analysis of the low-temperature regime at the compositional region near the magnetic-nonmagnetic crossover.

II. EXPERIMENTAL DETAILS

A. Instruments

The specific heat measurements in the range $0.2 < T < 6$ K were performed at the Instituto de Ciencia de Materiales de Aragón on a fully automated quasiadiabatic calorimeter[16] refrigerated by adiabatic demagnetization of a paramagnetic salt[17,18] using the heat pulse technique and germanium thermometry over the whole temperature range. Small ingots of around 0.5 g weight were used for the measurement, mixed with Apiezon N grease to achieve good thermal contact between the sample and the calorimetric set (heater and thermometer) even at the lowest temperature. The calorimeter is equipped with a mechanical switch that allows temperatures down to 0.2 K to be reached. The absolute accuracy of the instrument has been estimated to be about 1%.

The calorimetric data between 2 and 300 K were obtained in a commercial Quantum Design microcalorimeter at the University of Cantabria using the relaxation technique. In this case, thin slab-shape samples 0.5 mm thick and weighing around 8 mg were used. Matching between both sets of data in the common temperature range is quite satisfactory.

B. Samples

The samples in the present work are those with $x=0.1$, 0.15, 0.2, 0.3, 0.4, 0.5, 0.6, 0.7, 0.8, and 0.9. They are all polycrystalline samples prepared by carefully melting together stoichiometric amounts of the appropriate high-purity starting elements in an arc-melting furnace under inert Ar atmosphere. Five melts were performed with flipping of the arc-melted button between melts in order to improve homogeneity.

TABLE I. Crystallographic data of the $CeNi_{1-x}Cu_x$ compounds obtained at 300 K from x-ray diffraction data.

x	Structure	a (Å)	b (Å)	c (Å)	V (Å^3)
0.1	CrB	3.800(4)	10.490(1)	4.355(7)	173.7(3)
0.15	CrB	3.814(3)	10.565(8)	4.390(5)	176.9(3)
0.2	FeB	7.267(4)	4.425(2)	5.598(3)	180.1(1)
0.3	FeB	7.280(3)	4.428(2)	5.602(2)	180.6(1)
0.4	FeB	7.304(2)	4.445(1)	5.624(2)	182.6(1)
0.5	FeB	7.324(4)	4.471(2)	5.646(3)	184.9(1)
0.6	FeB	7.354(1)	4.500(5)	5.658(5)	187.2(1)
0.7	FeB	7.369(4)	4.506(2)	5.674(2)	188.4(1)
0.8	FeB	7.383(4)	4.528(2)	5.688(3)	190.2(2)
0.9	FeB	7.410(3)	4.543(1)	5.682(2)	191.3(1)

The crystalline structures of the $CeNi_{1-x}Cu_x$ compounds studied have been determined by x-ray diffraction at 300 K. The alloys with $x > 0.15$ crystallize in the FeB-type orthorhombic structure (*Pnma* space group), whereas the alloys with $x \leqslant 0.15$ crystallize in the CrB-type orthorhombic structure (*Cmcm* space group).[15] Both crystalline structures are built from Ce trigonal prisms (with a transition metal in the center). The two structures only differ in the relative disposition of the trigonal prisms, which is the reason why Ce-Ce and Ce-(Ni,Cu) distances evolve continuously from one structure to the other.[19]

The Rietveld analyses were performed considering Ni and Cu atoms randomly distributed on the same 4*c* site while the Ce lies on the other 4*c* site.

The narrowness of the x-ray peaks of the as-quenched sample spectra guarantees the good crystallization of the samples except for the Cu-rich ones, i.e., $x=0.8$ and 0.9, which showed a broadening of the diffraction peaks. A high-vacuum annealing at 425 °C (just below the melting point of CeCu) for one week was carried out on the samples with $x > 0.2$. Noticeable narrowing of the peaks was induced only for $x=0.8$ and 0.9 samples, whereas no significant modifications were observed for any of the other compositions.

The compounds with compositions close to the FeB-CrB-type structure change ($x=0.1$, 0.15, and 0.2) present signs of a mixture of FeB and CrB phases for the as-quenched preparations. The stabilization of the proper structure in each case was reached with a high-vacuum annealing at 440 °C for one week.

Table I summarizes the crystallographic data derived from the Rietveld refinements at 300 K for the studied compounds. The cell volume increases with the Cu content; the evolution is quite similar to that reported for $CeNi_yPt_{1-y}$;[20] both these sets of data are plotted in Fig. 1.

In order to get a better characterization of the microstructure of the samples, a scanning electron microscopy (SEM) study has also been performed.

The intensity of backscattered electron images taken with a SEM is proportional to the local atomic number of the sample. Therefore, these backscattered electron images yield

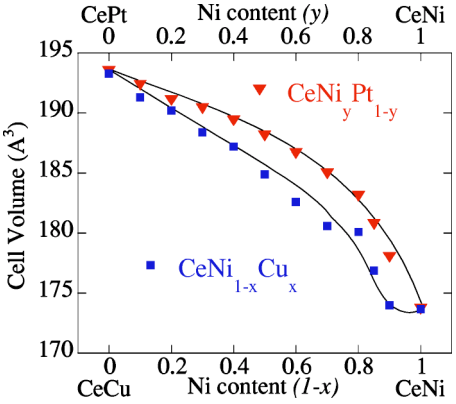

FIG. 1. Cell volume derived from x-ray diffraction for $CeNi_{1-x}Cu_x$ together with that for $CeNi_yPt_{1-y}$. The drawn lines are just a visual guideline.

semiquantitative information about composition homogeneity in a sample. Samples were prepared for SEM observations by using grinding paper disks of different grain sizes and final polishing with diamond paste. The SEM backscattered electron images were produced with a JEOL electron microscope at the University of Cantabria. Magnifications between 350 and 2000 were reached and quantitative electron probe microanalysis techniques were used to verify the chemical composition of the phases. We used secondary electron images to distinguish composition fluctuations from physical voids in the sample by comparing them with the backscattered electron images.

The backscattered electron images revealed that most of the sample volume consists of a matrix with the expected nominal composition in each case. Electron probe microanalysis measurements revealed that this matrix is homogeneous in all the scanned regions ($\sim 5\ \mu m^2$). We observed that as Cu concentration increases, samples tend to be very brittle and so the tendency to present cracks in the surface becomes more important.

III. RESULTS

The specific heat measurements performed in the temperature range 0.2 to 300 K on the compositions with FeB-type structure ($x > 0.15$) and also the isostructural YNi are shown in Fig. 2(a). The temperature dependence of C_P for YNi can be accounted for if an electronic term and a lattice one following the Debye function are taken into consideration. The fit of these data yields the values $\gamma = 5$ mJ/K^2 mol and $\theta_D = 250$ K, which are in good agreement with previous results.[21] Figure 2(b) displays the temperature dependence of the specific heat for the compositions with CrB-type structure ($x \leqslant 0.15$) together with the already reported data for the specific heat of CeNi and the isostructural nonmagnetic LaNi compound.[22] In that case, the temperature dependence of C_P for LaNi follows a Debye function with $\gamma = 5$ mJ/K^2 mol and $\theta_D = 190$ K.[22]

The inset of Fig. 2(b) shows the low-temperature region (from 0.2 to 6 K) of the total specific heat. The origin and nature of the anomalies shown here will be explained later on.

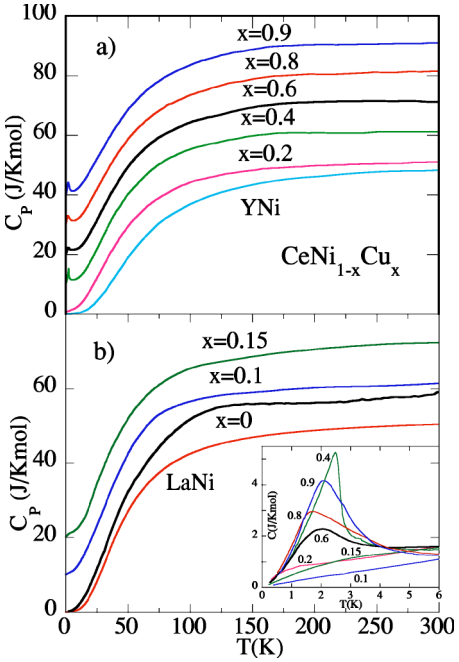

FIG. 2. (a) Temperature dependence of the specific heat for $CeNi_{1-x}Cu_x$ compounds with $x > 0.15$ and YNi. The YNi data has been fitted (solid line) considering a Debye and an electronic term (see text for details). (b) The specific heat for $x \leqslant 0.15$ compounds and LaNi. The CeNi and LaNi data were taken from Ref. 22. The data corresponding to different compounds have been shifted for clarity. The inset in Fig. 2(b) shows the total specific heat in the low-temperature regime.

A. Estimate of the electronic coefficient γ

The value of the linear electronic coefficient of the specific heat (γ) has been taken as the extrapolation of the linear part of the C_P/T vs T^2 curves at zero temperature, according to the law $C_P = \gamma T + \beta T^3$ followed at low temperatures, thus overlooking any anomalous contribution. The values obtained in this way are indicative of the electronic correlation enhancement, i.e., how far the corresponding compound is from the free-electron picture. Figure 3 illustrates this extrapolation for some selected compositions of the series. The

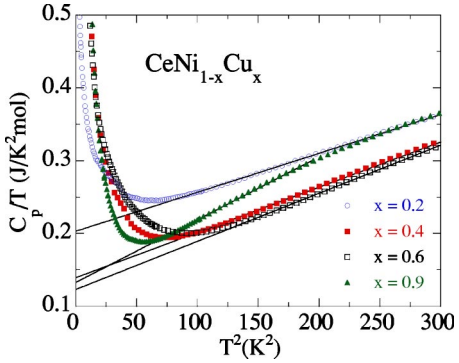

FIG. 3. Specific heat plotted as C_P/T vs T^2 showing the temperature range with a linear behavior whose extrapolation to $T = 0$ K allows the estimation of the electronic specific heat coefficient γ. Only some compositions are presented for clarity.

TABLE II. Magnetic characteristics of the compounds studied: Critical temperature (T_C); reduced magnetic entropy at T_C [$S_{mag}(T_C)/R \ln 2$]; linear electronic specific heat coefficient (γ); magnetic moment per Ce ion (μ) obtained from neutron diffraction analysis (Ref. 9); Kondo temperature (T_K) estimated from (i) the magnetic entropy (S_{mag}), (ii) the magnetic susceptibility ($\theta_P/10$) (Ref. 19), (iii) quasielastic neutron scattering (QENS) (Ref. 9), and (iv) the minimum in the electrical resistivity ($T_{\rho_{min}}/5$) (Ref. 19).

Compound	T_C (K)	$S_{mag}(T_C)$ (units of $R \ln 2$)	T_K S_{mag}	T_K QENS	T_K $\theta_P/10$	T_K $T_{\rho_{min}}/5$	γ (mJ/K^2 mol)	μ (μ_B)	Crystal electric field Δ_1, Δ_2 (K)
$CeNi_{0.1}Cu_{0.9}$	2.9	0.67	4.3	0.7	0.4		131	1	44, 105
$CeNi_{0.2}Cu_{0.8}$	3.0	0.58	4.8	1	0.1	1.9	117		47, 128
$CeNi_{0.3}Cu_{0.7}$	3.1	0.45	6.1		0.8	2.4	114		50, 116
$CeNi_{0.4}Cu_{0.6}$	2.7	0.46	6.0	2	1	2.8	112	0.6	49, 120
$CeNi_{0.5}Cu_{0.5}$	2.5	0.58	4.6		1.4	3.7	151	0.51	55, 146
$CeNi_{0.6}Cu_{0.4}$	2.6	0.60	4.7		1.7	4.7	154		62, 135
$CeNi_{0.7}Cu_{0.3}$	2.2	0.48	4.8				176		50, 116
$CeNi_{0.8}Cu_{0.2}$	1.8	0.19	6.6		4.1	7.2	206		51, 115
$CeNi_{0.85}Cu_{0.15}$			8.2		6	4.5	217		46, 100
$CeNi_{0.9}Cu_{0.1}$			13.8				150		67, 159
CeNi			140 (Ref. 22)				65 (Ref. 22)		

differences over the series are clearly seen both in the size of the C_P/T values and in the slopes of the C_P/T vs T^2 data, which correspond to the differences in the Sommerfeld coefficient (γ) and the Debye temperature (θ_D), respectively. Table II reports the values of γ obtained for all the compositions. According to the reported values (130–220 mJ/K^2 mol) these samples can be considered as moderate heavy fermions. The compositional dependence of γ is plotted in Fig. 4. We have shown in the same figure the dependence of γ on composition for $CeNi_yPt_{1-y}$,[23] another Ce system typifying the evolution from a localized magnetic state to a delocalized one according to the Doniach diagram.[24] In the latter case, the value of the γ coefficient increases when the Ni content does (increasing hybridization) and reaches a maximum value of more than 200 mJ/K^2 mol around the crossover where the change from a magnetic localized regime to a delocalized one takes place. Once the $4f$ delocalization is predominant, the γ value decreases with increasing Ni concentration.

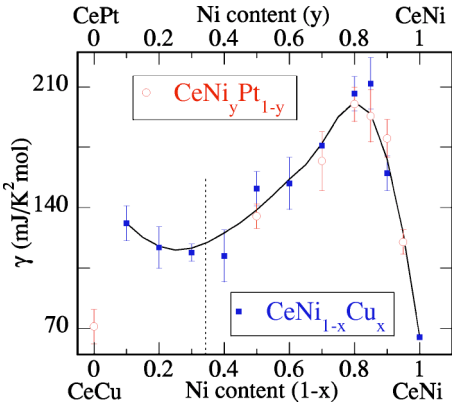

FIG. 4. Electronic specific heat coefficient (γ) for $CeNi_{1-x}Cu_x$ series as a function of Ni composition ($1-x$) and for $CeNi_yPt_{1-y}$ series as a function of Ni (y). The solid line is drawn as a guide only. The dashed lines set the crossover between the two compositional regimes defined in the text.

Returning to the γ evolution for the $CeNi_{1-x}Cu_x$ system displayed in the same plot, we became aware of the coincidence of the γ variation between the two series for Ni content larger than 0.5, whereas the compounds closer to CeCu follow a different trend from the $CeNi_yPt_{1-y}$ series. Thus, that comparison allows dividing the behavior of the series into two main composition regimes. Hence, the first regime would range from CeCu to $CeNi_{0.4}Cu_{0.6}$, where the values of γ do not significantly change. This region corresponds to the composition regime where the evolution from an AFM (CeCu) to an FM ($CeNi_{0.4}Cu_{0.6}$) ground state occurs, giving rise to complex ordered spin structures as has been established from neutron diffraction.[9] This evolution is considered to be caused by the enhancement of the ferromagnetic interactions closely related to the change in the density of states at the Fermi surface driven by the differences in d-electron density between Cu and Ni,[25] and it has been also found in similar $RNi_{1-x}Cu_x$ series with light[26] and heavy rare-earth elements.[27]

The evolution from $CeNi_{0.4}Cu_{0.6}$ to CeNi defines the second regime. Once the FM ground state sets in, the competition between RKKY, predominantly ferromagnetic, and Kondo interactions leads the system from a magnetic localized to a delocalized Pauli paramagnetic state (CeNi), and this competition defines the second regime. In that regime, the coefficient γ is enhanced for compounds with increasing hybridization favored by the decreasing cell volume, reaching values of more than 200 mJ/K^2 mol around the $x=0.15$ composition.

Let us come back to the cell volume variations of both series displayed in Fig. 1. In spite of the change in crystallographic structure existing in $CeNi_{1-x}Cu_x$, the cell volume evolves similarly for both series, both CePt and CeCu having nearly the same value of the cell volume. They do, however, have to be distinguished. While in $CeNi_{1-x}Cu_x$ the random substitution on the nonmagnetic site Ni-Cu not only changes the cell volume but also modifies the electronic state (by changing the number of conduction electrons), in the $CeNi_yPt_{1-y}$ case the Ni-Pt substitution modifies only the cell

volume. However, the evolution of γ is the same in both series in the thus defined second regime in $CeNi_{1-x}Cu_x$. The evolution of γ was explained in $CeNi_yPt_{1-y}$ as driven by the competition between RKKY and Kondo interactions under an internal molecular field[23] according to

$$\gamma \propto \frac{T_K}{T_K^2 + H^2}$$

where H is the Zeeman energy of the magnetic moment associated with a Ce^{3+} ion within the molecular field created by the other ions.

Then it is deduced from the previous comparison that the electronic effects do not play a predominant role in the balance between RKKY and $4f$ conduction band hybridization of the second regime. It can thus be concluded that the driving parameters of the γ behavior in this region are the interatomic distances rather than the electronic effects.

B. Estimate of C_{mag}

The magnetic contribution to the specific heat C_{mag} has been estimated for all the compounds by taking as the lattice contribution of each magnetic compound that of the isomorphous nonmagnetic one after taking into account the mass corrections.[28] Thus, the specific heat of LaNi (Ref. 21) has been taken as the nonmagnetic reference for the CrB-type structure compounds ($x=0.1$ and 0.15) while for the rest of the compositions (FeB-type structure) the specific heat of YNi was used. Using this procedure, C_{mag} reflects any effect related to the magnetic order transition and/or the temperature dependence of the electronic term.

1. C_{mag} in the low-temperature regime

Figure 5 displays C_{mag} as a function of the temperature in the low-temperature range for both regimes as defined in the previous section.

Thus, Fig. 5(a) illustrates the region $1>x>0.6$ where the evolution from an AFM to a FM ground state occurs due to the modifications of the positive and negative RKKY interactions. Figure 5(b) shows C_{mag} for compounds with $x<0.6$, where the magnetic ground state evolves from ferromagnetism to a Pauli paramagnetic state (CeNi).

Starting from the Cu-rich side, $CeNi_{0.1}Cu_{0.9}$ shows an anomaly at the critical temperature (T_C) corresponding to the antiferromagnetic transition ($T_N=2.5$ K) defined as the inflection point above the maximum of the C_{mag} curve. The anomaly becomes broader and its maximum value decreases as Ni content increases; it is significantly reduced for the $x=0.6$ compound, which shows a broad hump centered at about 2 K. It is worth noting the smooth variation of C_{mag} above the ordering temperature for these compounds. These effects are related to the existence of a short-range magnetic order well above T_N. In fact, the competition between positive and negative interactions leads to complex ordered spin structures, as was corroborated by neutron diffraction.[9] In addition, quasielastic neutron scattering (QENS) carried out in the $x=0.9$, 0.8, and 0.6 compounds[9] indicated a supplementary inelastic Gaussian contribution persisting up to

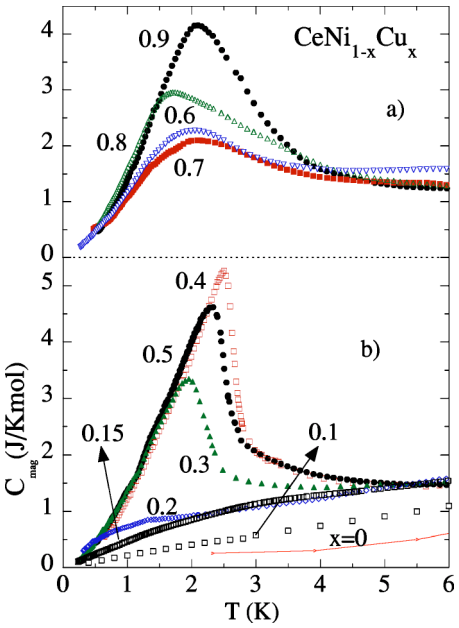

FIG. 5. C_{mag} versus temperature in the low-temperature regime plotted separately for the two composition regions defined: (a) $0.9 \leqslant x \leqslant 0.6$ or region where the system evolves from AFM to FM ground state; (b) $x \leqslant 0.6$ or region where hybridization effects and disorder are predominant (for details see text).

$\sim 3T_C$, which becomes more important as Cu content increases (i.e., as the exchange interactions became more significant). All these features support the predominant role played by RKKY interactions in setting the magnetic ground state in this regime.

We note a perceptible change in C_{mag} between $x=0.6$ and 0.5. Instead of a hump, $CeNi_{0.5}Cu_{0.5}$ exhibits a clear λ-type anomaly, with a critical temperature $T_C=2.3$ K. This anomaly becomes even sharper for $CeNi_{0.6}Cu_{0.4}$ and shifts slightly up to $T_C=2.5$ K. For the following compounds, the anomaly broadens and its maximum value decreases with increasing Ni content. Thus, for compositions with $x<0.2$, the anomaly in C_{mag} cannot be distinctly defined.

The temperature corresponding to the maximum of the magnetic specific heat coincides with the freezing temperature (T_f) determined by ac magnetic susceptibility measurements, which for the compounds in this second regime was associated with a "spin-glass-like" state developing at temperatures above the long-range ferromagnetic order.[11,29] Microscopic studies performed with μSR in order to shed light on the nature and origin of these transitions suggested an intermediate inhomogeneous magnetic state above T_f evolving into a long-range ordered state at lower temperatures. However, from the specific heat point of view, no other transitions were observed at temperatures below the maxima. This feature agrees with the idea of a continuous evolution (better than a second-order phase transition) to the long-range ordered state found from neutron and muon results at low temperatures.[9,13] Earlier calorimetric studies presented in $CeNi_{0.4}Cu_{0.6}$ revealed a very narrow peak at 1 K.[10] The actual measurement in this composition is identical to the already published one except for that feature. We should bear in mind that Ref. 10 was an in-depth study on one composi-

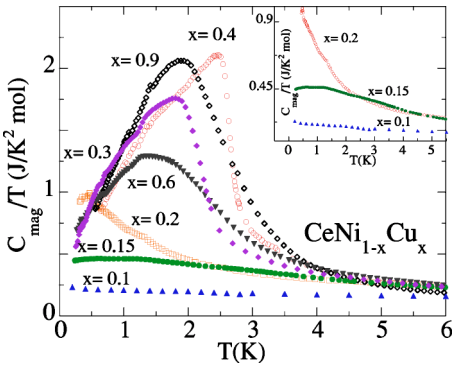

FIG. 6. C_{mag}/T vs T representation of the specific heat for $CeNi_{1-x}Cu_x$ in the compositions studied. The inset shows the variation for the compounds near the magnetic-nonmagnetic crossover $x=0.1$, 0.15, and 0.2.

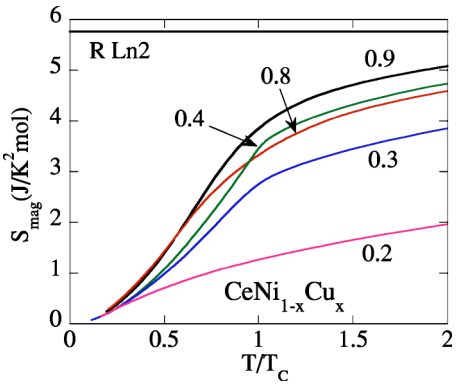

FIG. 7. Magnetic entropy S_{mag} for $CeNi_{1-x}Cu_x$ versus reduced temperature (T/T_C) for some selected compounds for clarity.

tion of the $CeNi_{1-x}Cu_x$ series and at that point when even the magnetic phase diagram of the series was unknown, we were not aware of the enormous relevance of a meticulous characterization of the samples. In fact, the sample reported in Ref. 10 was melted in an induction furnace and its degree of inhomogeneity was not as well characterized as in the present study.

Taking a look at the very-low-temperature side of the C_{mag}/T vs T curves (Fig. 6), we can observe an almost constant behavior for $CeNi_{0.85}Cu_{0.15}$ and $CeNi_{0.9}Cu_{0.1}$. This fact indicates the Fermi-liquid character of these compounds. It should be remarked that the Fermi-liquid theory should only be applied at very low temperatures where it describes the low-lying excitations of the quasiparticles (interacting fermions). However, it is usually assumed that this label can be extended to compounds presenting a constant electronic specific heat and magnetic susceptibility coefficient and a T^2 dependence of the electrical resistivity. This is the case of the C_{mag}/T corresponding to the $x=0.1$ and 0.15 compounds.

In f-electron compounds, strong electronic correlations can lead to anomalous low-temperature properties indicating that the system changes from a nonmagnetic to a magnetic ground state as a certain parameter such as concentration or pressure is tuned. Typically, the NFL behavior is associated with a diverging specific heat C_{mag}/T when approaching $T=0$ K, while the Fermi-liquid theory predicts a constant value.[2]

In $CeNi_{1-x}Cu_x$, the whole set of measurements traces a crossover from magnetic order to Pauli paramagnetic behavior, thereby crossing some critical concentration range where long-range order is expected to vanish. Therefore, one might ask if NFL behavior might arise in this system. In that sense, what is remarkable is the divergence of the C_{mag}/T curve at low temperatures for the $x=0.2$ compound.

We are tempted to attribute the origin of this divergence to its being the critical concentration where long-range magnetic order is suppressed, then presenting a NFL behavior as in other series exhibiting, in principle, a similar scenario. However, the existence of a transition at lower temperature cannot fully be ruled out. The low-temperature dependence of C_{mag}/T must be carefully analyzed in this case. In fact, as we mentioned in the Introduction, very-low-temperature studies by both macroscopic (ac and dc measurements[14]) and microscopic (μSR) techniques[13] in the compositions around $x=0.2$ revealed that the magnetic moments are not yet exhausted. However, long-range magnetic order, if it exists, cannot be detected by neutron diffraction (within the resolution of the available experiments) since we are dealing with very reduced values of the magnetic moment. Both experiments point toward some kind of short-range ordered states and reveal evidence of spin-glass arrangements even for the $x=0.1$ compound.[15] Thus, on the basis of all these results we have to discard an intrinsic electronic effect leading to a NFL or quantum phase transition around the $x=0.2$ compound. The divergence in C_{mag}/T could be related to the existence of a small anomaly at lower temperatures as was found at very low temperature in ac susceptibility measurements.[14]

2. Low-temperature magnetic entropy

The magnetic entropies have been calculated from

$$S_{mag} = \int_0^T \frac{C_{mag}}{T} dT$$

and are shown in Fig. 7 versus the reduced temperature (T/T_C) for the most significant compounds.

The first point to be discussed in the entropy analysis is the shape of these curves below T_C. As has been pointed out in other series such as RGa_2 (Ref. 30) and RNi_2Si_2 (Ref. 31), this shape is closely related to the magnetic structure and the thermal demagnetization processes. The more simple the structure is with well-defined anisotropy, the sharper the increase of the entropy is, defining a clear change of slope at T_C. This is the case shown in Fig. 7 where for the AFM complex structures ($x=0.8$ and 0.9) a slow and progressive increase is observed, whereas for the FM one ($x=0.4$) the increase is sharper and a knee is observed at T_C. It must be stressed, however, that in this $CeNi_{1-x}Cu_x$ series these variations are quite smooth even in the case of FM compounds, indicating a high degree of magnetic disorder.

In all the compounds the magnetic entropy at T_C is lower than $R\ln 2=5.76$ J/K mol, the value expected from a doublet ground state, which is the one presented by the Ce^{3+} ion under an orthorhombic framework. The reasons for such a reduction are at least two. The first one is the complexity of

the magnetic order with the existence of short-range interactions above T_C; this should be the main effect in compounds close to the CeCu limit. The value of the entropy at T_C decreases as the structure become more complex (RKKY competing interactions being the predominant effect). The second is the Kondo effect, which reduces the value of the magnetic moment that is the dominant effect once the ferromagnetic order is established ($x<0.6$) and the Kondo interactions become more important. This reduction of the magnetic moment has been confirmed by neutron and muon experiments.[10,13]

From this last assumption a T_K value can be estimated considering the reduction of the magnetic entropy at T_C from the value of $R\ln 2$.[32] Using a simple two-level model with an energy splitting of $k_B T_K$, we can calculate the reduced entropy at T_C as

$$\frac{\Delta S}{R} = \ln\left[1+\exp\left(\frac{-T_K}{T_C}\right)\right] + \frac{T_K}{T_C}\left[\frac{\exp(-T_K/T_C)}{1+\exp(-T_K/T_C)}\right].$$

This expression must be applied for transitions at T_C to long-range magnetic order which is not really the case in our compounds with $x\leqslant 0.6$. In this case the specific heat anomaly at T_C is related to the spin freezing temperature. However, the frozen state in these samples is a cluster glass with ferromagnetic correlations inside the clusters. So, even if some fraction of the entropy is invested in the disorder among the clusters, this approach can give us an estimate of the Kondo temperatures in order to follow their compositional evolution.

For the compounds with no anomaly in $C_{\mathrm{mag}}(x<0.2)$, the estimation of T_K requires another kind of analysis. From the Sacramento and Schlottmann calculations for a $J=1/2$ impurity,[33] one could estimate T_K as the value at which 45% of the total $R\ln 2$ entropy is recovered.

Taking into account the perturbation induced by the short-range order correlations and the two different methods used to estimate the T_K values, these results must be looked at with care.

Table II summarizes the values obtained for T_K in each composition. In the same table we also present the values of T_K estimated from susceptibility[19] as $|\theta_P|/10$, QENS,[9] and resistivity as $T_{\rho\min}/5$.[19]

It is clear that the right estimate of T_K comes from QENS,[9] where the quasielastic signal is directly related to the Kondo temperature. The values of T_K obtained from the magnetic entropy are clearly overestimated due to the entropy associated with cluster-glass formation.

The most interesting feature in all these estimates of T_K is that, in spite of the different magnitudes due to the different time scales of the techniques,[23,34,35] the same relative variation of T_K is found with increasing Ni content.

C. C_{mag} above T_C

Apart from short-range order correlations that might be present above the critical temperature, the contribution to C_{mag} above T_C arises from the crystal electric field (CEF). Due to the low-symmetry site occupied by the Ce^{3+} ions in this system, the $J=5/2$ multiplet splits into three doublets,

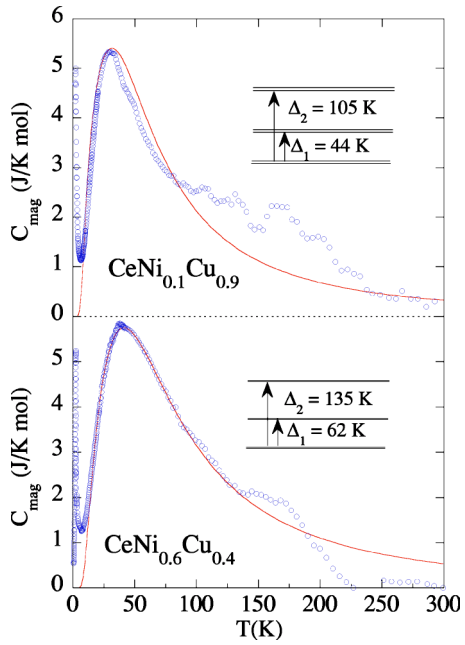

FIG. 8. Magnetic contribution to the specific heat as a function of temperature for $CeNi_{0.1}Cu_{0.9}$ and $CeNi_{0.6}Cu_{0.4}$. Solid lines correspond to the paramagnetic CEF contribution (see text). The arrows indicate the main transitions in the CEF level scheme.

with the excited states separated from the ground state by energy gaps Δ_1 and Δ_2. A Schottky-type anomaly is then expected. The hump around 50 K appearing in all the studied compounds of this series has been analyzed considering this CEF scheme. The values Δ_1 and Δ_2 that correspond to the best Schottky-type fit to C_{mag} are listed in Table II.

The values obtained for the energy gaps are similar for all the compositions with FeB-type structure. Moreover, the level scheme found for the CrB compositions ($x=0.15$ and 0.1) is close to that corresponding to the FeB-type ones. This result indicates that the Ni—Cu dilution does not significantly modify the CEF splitting over the series.

Special attention must be paid to the CrB compositions. On the one hand, the presence of Schottky-type anomalies supports the fact that the magnetic moment in Ce^{3+} remains localized still for those concentrations close to CeNi. On the other hand, the values found for the samples with CrB- and FeB-type structures reveal that the change in the structure does not introduce significant changes in the CEF sensed by the Ce^{3+} ions. This fact indicates the similarity between both structures as was already pointed out in Sec. II B.

In contrast, it is worth noting that for the intermediate valence compound CeNi, a broad contribution centered around 140 K was observed in previous works,[22] it being related to spin fluctuations present in compounds close to the onset of ferromagnetism.

The magnetic contribution to the specific heat in the paramagnetic range together with the best fit obtained for the Schottky anomaly and the associated level scheme are illustrated in Fig. 8 as an example for $x=0.9$ and 0.4.

Finally, the magnetic entropy S_{mag} calculated from the experimental C_{mag} variation for the $0.2<T<300$ K temperature range is shown in Fig. 9 for some selected compounds.

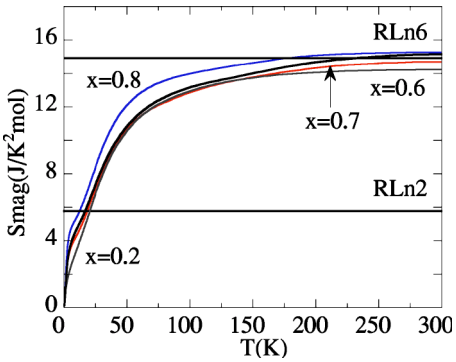

FIG. 9. Magnetic entropy S_{mag} versus temperature extended to the whole temperature range studied for $CeNi_{1-x}Cu_x$.

For increasing temperature, S_{mag} progressively increases due to the thermal population of the excited CEF levels, reaching saturation around 250 K. The saturation values are close to the theoretical value $R \ln 6 = 14.89$ J/K^2 mol, as corresponds to the magnetic entropy of a Ce^{3+} ion with a total angular momentum $J = 5/2$.

IV. DISCUSSION

The actual calorimetric study has provided useful information about the complex magnetic ground state found in this system. This section is devoted to analyzing the behavior of the series, based on both the present and the previous studies carried out so far.

First, we must remember the division of the series into two regimes with respect to the heat capacity findings. Although the competing interactions are present throughout the series, the heat capacity reflects that the interplay of the interactions and their magnitude are tuned by the composition. Thus, we have defined a first regime where the competing exchange interactions are predominant $(0.9 \leqslant x < 0.6)$, giving rise to a change from antiferromagnetism to ferromagnetism. The second regime is characterized by the increasing Kondo effect driven by the decreasing cell volume. As the Kondo effect becomes more important, the Ce magnetic moments become smaller and the effective magnetic interaction decreases.

In this second regime the general behavior is the same as that expected for a Kondo lattice system and the electronic coefficient γ evolves similarly as in the $CeNi_yPt_{1-y}$ series,[23] a clear example of a Doniach-predicted behavior.

The maximum value of γ corresponds to the composition where Kondo interactions overcome the molecular field effects and then long-range magnetic order is hard to reach. For compounds presenting higher Ni content, γ behaves as in the nonordered heavy fermion compounds, $\gamma \propto 1/T_K$. In our case, however, important magnetic disorder effects still prevail. Furthermore, the magnetic moments are not completely exhausted and they can arrange at very low temperatures.

The complex magnetic behavior and the evolution of the interactions in this series can be condensed into the sketch picture displayed in Fig. 10.

Previous bulk data suggested the existence of a spin-glass-like phase (cluster glass in Fig. 10) appearing in a certain compositional range of this series at the freezing temperature T_f.[11,29] In addition, long-range ferromagnetic order at very low temperatures has been confirmed by neutron diffraction and μSR studies at least down to the composition with $x = 0.2$.[13,36] The low-temperature specific heat for these compounds exhibits marked anomalies at the freezing temperature T_f detected by ac susceptibility. The shape of these anomalies, however, differs from what is expected around the freezing temperature in a canonical spin glass.

So far, a lot of experimental data on the magnetic heat capacity behavior of "spin-glass" systems are available and few analytical expressions have been used to reproduce the data for the different samples.[37,38] Furthermore, the "spin-glass" label has been used to refer to many different situations ranging from the canonical spin glass (i.e., individual spins) to magnetic ground states close to superparamagnetism (i.e., noninteracting magnetic spin clusters). That is the reason why some of the spin-glass properties do not seem to be universal. In particular, it is usually assumed that the magnetic contribution to the specific heat shows no sharp anomaly at the freezing temperature, as found in other heavy fermion intermetallic compounds with spin-glass-like behavior: U_2PdSi_3 (Ref. 39), URh_2Ge_2 (Ref. 40), and more recently $CeNi_2Sn_2$ (Ref. 41). Our data do not conform with this common phenomenology although the magnetic macroscopic measurements clearly point to a spin-glass-like behavior.

Furthermore, the magnetic entropy reached at the spin freezing temperature is estimated to be 45–60 % of the theoretical value $R \ln 2$ corresponding to the full degeneracy of the magnetic ground state (see Table II). That percentage is slightly higher than those reported for the crystalline dilute spin-glass systems MnCu or AuFe (22–33 %),[42] even taking into account the entropy reduction due to the Kondo effect in our samples. Compared with our data, a similar specific heat and magnetic entropy behavior was also found in amorphous $Gd_{33}Al_{67}$ (Ref. 43) and $Er_{50}Ni_{50}$ (Ref. 44) alloys. In addition, for those compounds the magnetic specific heat showed a $T^{3/2}$ temperature dependence, indicating a collective excita-

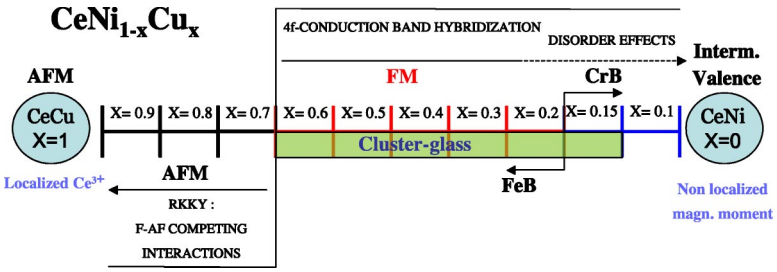

FIG. 10. Schematic evolution of both the magnetic behavior and structural characteristics of $CeNi_{1-x}Cu$. The two different regimes deduced from these calorimetric studies are indicated together with the predominant interaction.

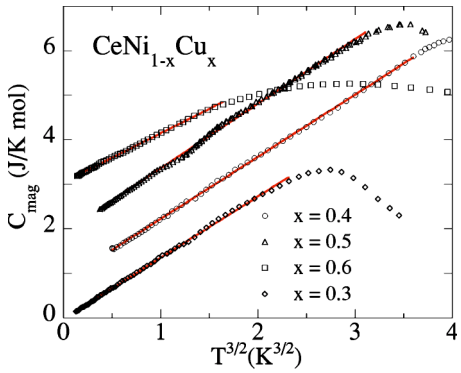

FIG. 11. Temperature dependence of the magnetic contribution to the specific heat C_{mag} for the FM compounds $x=0.3$, 0.4, 0.5, and 0.6 in the form C_{mag} versus $T^{3/2}$. The data corresponding to different compounds are shifted for clarity.

tion. These results indicate that ferromagneticlike spin waves can be excited in these amorphous alloys, although the overall magnetic structure is not ferromagnetic but rather spin glass. Figure 11 displays the temperature dependence of our magnetic specific heat in the form C_{mag} versus $T^{3/2}$ for the ferromagnetic compounds with $x=0.3$, 0.4, 0.5, and 0.6. It is clear that C_{mag} follows the $T^{3/2}$ dependence up to about $0.7T_f$ in a similar manner as observed in the amorphous compounds cited above. The existence of these ferromagnetic correlations yields a faster enhancement of the magnetic entropy than that of a canonical spin glass (linear with temperature). Thus, the maximum value of the specific heat has to be reached at a lower temperature than the $1.6T_f$ expected value,[37,38] as happens in our series.

Neutron diffraction experiments at very low temperature have been conclusive in ascertaining the existence of long-range ferromagnetic order in $x=0.6$, 0.5, and 0.4 compounds.[9,36] Neutron scattering is primarily a probe of long-range correlations. On the other hand, μSR spectroscopy is a much more local probe than neutron scattering, and needs no large coherence length. Consequently, it is particularly sensitive to short-range order and other forms of disordered magnetism.[45] Our μSR results indicate the existence of an inhomogeneous magnetic state at temperatures above the freezing temperature T_f (seen by ac susceptibility) that runs into the paramagnetic regime. The basic feature of this intermediate state is the coexistence of ordered and nonordered fractions. The latter decreases as the temperature is lowered until T_f is reached. Below T_f, long-range order, from the μSR perspective,[45] prevails. Nevertheless, it must be stressed that this long-range ordered state detected by muons presents strong local magnetic disorder as reflected by the wide field distribution on the muon site arising from those analyses. This distribution leads to the fast damping of the oscillatory pattern observed in the series.[13]

It is worth remembering the difference in the time window for the study of spin dynamical processes when comparing the different experimental techniques used so far (i.e., ac susceptibility, specific heat, neutron diffraction, and μSR spectroscopy). Each technique can access a different characteristic range of the rate of spin fluctuations and hence provides different information concerning dynamical processes developing in the system. The combination of all the techniques, however, yields a complete dynamical picture of the system since μSR bridges the gap between neutron scattering on the one side and bulk magnetic measurements on the other.[45]

Considering our experimental results as a whole, we can propose a convenient description of our system. Although x-ray and neutron diffraction and scanning microscopy reflect a clear homogeneity of the samples at the micrometric level, we can be sure that inhomogeneities in the random distribution of Cu and Ni appear at the nanometric scale. When temperature is lowered from the paramagnetic state, zones or clusters of magnetic moments develop due to the increasing short-range magnetic interactions. These clusters freeze at T_f, losing their dynamical aspect. At lower temperatures the magnetic clusters interact among one another and percolate giving rise to a long-range ferromagnetic state at very low temperatures, in agreement with the ferromagnetic excitations detected by specific heat below T_f. This percolative process scenario, reminiscent of that proposed by Dagotto in manganites,[46] is also present in many substitutional systems such as semiconductors, high-T_C superconductors, etc.[47] The $CeNi_{1-x}Cu_x$ is, thus, a clear example of a strongly correlated electron system presenting a percolative scenario.

In the compound with $x=0.2$, the inhomogeneous magnetic state, where ordered and nonordered fractions coexist, extends over a wider temperature range. A fully long-range ordered state has been detected by μSR and ac susceptibility only below $T\sim 0.5$ K.[13,14] At this point we must remember that this compound was reported to be on the crossover point of the localized-nonlocalized magnetism.[11] In fact, the specific heat measurements do not show any sharp transition as in the other compounds. Furthermore, recent neutron diffraction studies do not detect any magnetic contribution within the experimental limits.[36] These results evidence how reduced the Ce magnetic moments are in this alloy. Being so close to the disappearance of the magnetic moment and regarding the C_{mag}/T behavior presented in the previous section, one could be tempted to look for a NFL behavior defining a QCP in this composition. In that sense, Fig. 12 shows the corresponding fits of C_{mag}/T for this compound to a $\log_{10} T$ law, as observed for the case of magnetic fluctuations[3,48,49] and a $T^{-1+\lambda}$ law as proposed by Castro Neto,[6] who considered the existence of Griffiths phases consisting of magnetic clusters embedded in a nonmagnetic matrix.

Although the agreement factor of these fits is comparable to other systems reported as non-Fermi liquids,[50] in the present case we have powerful reasons to discard this option. On the one hand, ac susceptibility shows the presence of a transition at very low temperatures as we pointed out above[14] and, on the other hand, the hysteresis loops in $x=0.15$ and 0.1 compounds observed at very low temperatures[15] suggest the existence of a "cluster-glass" state even for those compounds that macroscopically behave as Fermi liquids with almost constant C_{mag}/T value.

In our opinion the scenario for this series has to be understood without considering a QCP situation, but rather as only a consequence of the increasing hybridization in an intrinsic inhomogeneous state that leads to a cluster-glass situation.

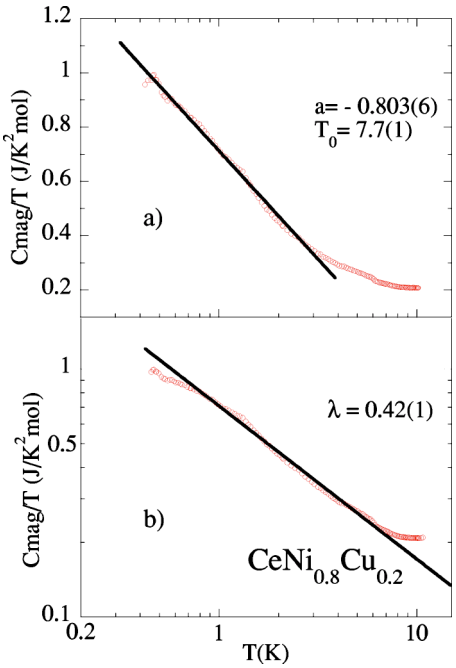

FIG. 12. (a) C_{mag}/T vs $\log_{10} T$ and (b) $\log_{10}(C_{mag}/T)$ vs $\log_{10} T$ plots for the $x=0.2$ compound. The reported a, T_0, and λ values are the parameters obtained from the (a) $C_{mag}/T \propto a \log_{10}(T/T_0)$ and (b) $C_{mag}/T \propto T^{-1+\lambda}$ laws.

The more important the reduction of the magnetic moment is, the lower is the stability of a long-range ordered state. This interpretation resembles the situation described by Coleman,[4,5] where the magnetic moments still persist in the NFL regime, as is the case in MnSi.[51]

The possibility of the scenario proposed here could be extended to other substitutional systems such as $UCu_{5-x}Pd_x$ (Refs. 52 and 53) and more recently $UPd_{2-x}Sn_x$ (Ref. 54) and $CePtSi_{1-x}Ge_x$ (Ref. 55) where intrinsic disorder effects were detected. This fact points out the importance of careful analysis of such systems close to the evanescence of the long-range magnetic order (the QCP). The quantum effects due to new electronic ground states must be confirmed by studies carried out in good single-crystal samples and avoiding substitutional effects.

V. CONCLUSIONS

$CeNi_{1-x}Cu_x$ is a complex system that presented many open questions concerning its magnetic behavior. The analysis of the specific heat has shed light on most of those intriguing experimental facts. In this way, it has been possible to distinguish two main concentration regimes: the first one close to the Cu-rich side, where the exchange interactions are predominant and the magnetic behavior resembles our findings in other $RNi_{1-x}Cu_x$ series [i.e., $NdNi_{1-x}Cu_x$ (Ref. 26)] leading to changes from AFM to FM; the second one with ferromagnetic behavior, but governed by Kondo interactions tending to reduce the Ce magnetic moment that vanishes in the CeNi compound in agreement with the Doniach model, in a similar way as already found in $CeNi_yPt_{1-y}$.[23,24] We have also carefully investigated the possible existence of a NFL behavior for compositions close to the apparent vanishing of the long-range order and its relation to a QCP. Considering the analysis of C_P alone, we can report an enhanced Fermi-liquid behavior (γ constant with temperature) for compounds with $x<0.2$, and a divergence in the C_P/T vs T plot for $x=0.2$ that could be reasonably well reproduced by NFL models. However, supplementary information obtained by ac and dc susceptibility measurements confirms the existence of hysteresis loops at low temperature indicating that the magnetic moments are not fully exhausted in those compounds. The QCP scenario is then not required to account for that behavior in this series.

A special effort has been made to understand the magnetic contribution of C_P related to the spin-glass state or the short-range magnetic ordered state. For this purpose we have considered previous μSR, neutron diffraction, and χ_{ac} results, which provide different time scales of those dynamical processes. The critical temperature T_C represents the temperature where ferromagnetic correlations are established, although full long-range order only occurs at lower temperatures. Considering the overall results it has been possible to propose a convenient description of our system. Its magnetic behavior can be fully described by the existence of interacting magnetic clusters that percolate, giving rise to a long-range magnetic state at very low temperatures.

Our results allow us to extend the large variety of examples of systems presenting intrinsic inhomogeneities that reach long-range magnetic order by percolating processes (semiconductors, manganites, high-T_C superconductors, etc.) to strongly correlated electron metals underlying those intrinsic disorder effects that cannot be avoided and are present in mixed or substitutional systems.

ACKNOWLEDGMENTS

This work was supported by the MAT2003-06815, the FERLIN-ESF program, and the Fundación Ramón Areces. N.M. and J.H.-A. acknowledge MEC for partial financial support. Fruitful discussions with G. M. Kalvius are also acknowledged. We are indebted to David Culebras for his invaluable technical assistance.

[1] E. S. R. Gopal, *Specific Heats at Low Temperatures* (Heywood Books, London, 1966).

[2] See, for instance, Proceedings of the Conference on NFL Behaviour in Metals, Santa Barbara, edited by P. Coleman, M. B. Maple, and A. J. Millis [J. Phys.: Condens. Matter 8, 48 (1996)].

[3] T. Moriya and T. Takimoto, J. Phys. Soc. Jpn. **64**, 960 (1995).

[4] P. Coleman, Physica B **259–261**, 353 (1999).

[5] A. Schröder, G. Aeppli, R. Coldea, M. Adams, O. Stockert, H.

von Löhneysen, E. Bucher, R. Ramazashvili, and P. Coleman, Nature (London) **407**, 351 (2000).
[6] A. H. Castro Neto, G. Castilla, and B. A. Jones, Phys. Rev. Lett. **81**, 3531 (1998).
[7] O. O. Bernal, D. E. MacLaughlin, H. G. Lukefahr, and B. Andraka, Phys. Rev. Lett. **75**, 2023 (1995).
[8] E. Miranda, V. Dobrosavljevic, and G. Kotliar, Phys. Rev. Lett. **78**, 290 (1997).
[9] J. I. Espeso, J. García Soldevilla, J. A. Blanco, J. Rodríguez Fernández, J. C. Gómez Sal, and M. T. Fernández Díaz, Eur. Phys. J. B **18**, 625 (2000).
[10] J. C. Gómez Sal, J. García Soldevilla, J. A. Blanco, J. I. Espeso, J. Rodríguez Fernández, F. Luis, F. Bartolomé, and J. Bartolomé, Phys. Rev. B **56**, 11 741 (1997).
[11] J. García Soldevilla, J. C. Gómez Sal, J. A. Blanco, J. I. Espeso, and J. Rodríguez Fernández, Phys. Rev. B **61**, 6821 (2000).
[12] J. C. Gómez Sal, J. I. Espeso, J. Rodríguez Fernández, N. Marcano, and J. A. Blanco, J. Magn. Magn. Mater. **242–245**, 125 (2002).
[13] N. Marcano, G. M. Kalvius, D. R. Noakes, J. C. Gómez Sal, R. Wäppling, J. I. Espeso, E. Schreier, A. Kratzer, Ch. Baines, and A. Amato, Phys. Scr. **68**, 298 (2003).
[14] N. Marcano, J. I. Espeso, J. C. Gómez Sal, L. Sánchez, G. M. Kalvius, C. Paulsen, and Ch. Sekine, Acta Phys. Pol. B **34**, 1477 (2003).
[15] N. Marcano, D. Paccard, J. I. Espeso, J. Allemand, J. M. Moreau, A. Kurbakov, C. Sekine, C. Paulsen, E. Lhotel, and J. C. Gómez Sal, J. Magn. Magn. Mater. **272–276**, 468 (2004).
[16] J. Bartolomé and F. Bartolomé, Phase Transitions **64**, 57 (1997).
[17] A. R. Miedema, R. F. Wielinga, and W. J. Huiskamp, Physica (Amsterdam) **31**, 1585 (1965).
[18] H. A. Algra, L. J. de Jongh, W. J. Huiskamp, and R. L. Carlin, Physica B & C **92**, 187 (1977).
[19] J. García Soldevilla, J. C. Gómez Sal, J. I. Espeso, J. Rodríguez Fernández, J. A. Blanco, M. T. Fernández Díaz, and H. Buttner, J. Magn. Magn. Mater. **177–181**, 300 (1998).
[20] D. Gignoux and J. C. Gómez Sal, Phys. Rev. B **30**, 3967 (1984).
[21] J. A. Blanco, J. C. Gómez Sal, J. Rodríguez Fernández, M. Castro, R. Burriel, D. Gignoux, and D. Schmitt, Solid State Commun. **89**, 389 (1994).
[22] D. Gignoux, F. Givord, R. Lemaire, and F. Tasset, J. Less-Common Met. **94**, 165 (1983).
[23] J. A. Blanco, M. de Podesta, J. I. Espeso, J. C. Gómez Sal, C. Lester, K. A. McEwen, N. Patrikios, and J. Rodríguez Fernández, Phys. Rev. B **49**, 15 126 (1994).
[24] S. Doniach, in *Valence Instabilities and Related Narrow Band Phenomena*, edited by R. D. Parks (Plenum, New York, 1976), p. 169.
[25] A. Hernando, J. M. Rojo, J. C. Gómez Sal, and J. M. Novo, J. Appl. Phys. **79**, 4815 (1996).
[26] J. García Soldevilla, J. A. Blanco, J. Rodríguez Fernández, J. I. Espeso, J. C. Gómez Sal, M. T. Fernández-Díaz, J. Rodríguez Carvajal, and D. Paccard, Phys. Rev. B **70**, 224411 (2004).
[27] D. Gignoux and J. C. Gómez Sal, J. Magn. Magn. Mater. **1**, 203 (1976).
[28] M. Bouvier, P. Lethuiller, and D. Schmitt, Phys. Rev. B **43**, 13 137 (1991).
[29] J. C. Gómez Sal, J. Rodríguez Fernández, J. I. Espeso, N. Marcano, and J. A. Blanco, J. Magn. Magn. Mater. **226–230**, 124 (2001).
[30] J. A. Blanco, D. Gignoux, J. C. Gómez Sal, J. Rodríguez Fernández, and D. Schmitt, J. Magn. Magn. Mater. **104–107**, 1285 (1992).
[31] J. M. Barandiarán, D. Gignoux, D. Schmitt, J. C. Gómez Sal, and J. Rodríguez Fernández, J. Magn. Magn. Mater. **69**, 61 (1987).
[32] H. Yashima, H. Mori, N. Sato, and T. Satoh, J. Magn. Magn. Mater. **31–34**, 411 (1983).
[33] P. D. Sacramento and P. Schlottmann, Phys. Rev. B **40**, 431 (1989).
[34] R. M. Galera, A. P. Murani, and J. Pierre, Physica B **156–157**, 801 (1989).
[35] D. Gignoux, A. P. Murani, D. Schmitt, and M. Zerguine, J. Phys. I **1**, 281 (1991).
[36] N. Marcano, Ph.D. thesis, University of Cantabria, 2004.
[37] K. Binder and A. P. Young, Rev. Mod. Phys. **58**, 801 (1986).
[38] J. A. Mydosh, in *Spin Glasses: An Experimental Introduction* (Taylor & Francis, London, 1993).
[39] D. X. Li, Y. Shiokawa, Y. Homma, A. Uesawa, A. Dönni, T. Suzuki, Y. Haga, E. Yamamoto, T. Honma, and Y. Onuki, Phys. Rev. B **57**, 7434 (1998).
[40] S. Süllow, G. J. Nieuwenhuys, A. A. Menovsky, J. A. Mydosh, S. A. M. Mentink, T. E. Mason, and W. J. L. Buyers, Phys. Rev. Lett. **78**, 354 (1997); S. Süllow, S. A. M. Mentink, T. E. Mason, W. J. L. Buyers, G. J. Nieuwenhuys, A. A. Menovsky, and J. A. Mydosh, Physica B **230–232**, 105 (1997); S. Süllow, S. A. M. Mentink, T. E. Mason, R. Feyerherm, G. J. Nieuwenhuys, A. A. Menovsky, and J. A. Mydosh, Phys. Rev. B **61**, 8878 (2000).
[41] C. Tien, J. J. Lu, and L. Y. Jang, Phys. Rev. B **65**, 214416 (2002).
[42] L. E. Wenger and P. H. Keesom, Phys. Rev. B **13**, 4053 (1976).
[43] J. M. D. Coey, S. von Molnar, and R. J. Gambino, Solid State Commun. **24**, 167 (1977).
[44] Y. Hattori, K. Fukamichi, K. Suzuki, H. Aruga-Katori, and T. Goto, J. Phys.: Condens. Matter **7**, 4193 (1995).
[45] G. M. Kalvius, D. R. Noakes, and O. Hartmann, in *Handbook on the Physics and Chemistry of Rare Earths* edited by K. A. Gschneidner and L. Eyring (North-Holland, Amsterdam, 2001), Vol. 32, p. 55.
[46] E. Dagotto, *Nanoscale Phase Separation and Colossal Magnetoresistance* (Springer-Verlag, Berlin, 2002); E. Dagotto cond-mat/0302550 (unpublished), and references therein.
[47] M. Mayr, G. Alvarez, and E. Dagotto, Phys. Rev. B **65**, 241202 (2002); G. Alvarez and E. Dagotto, cond-mat/0305628 (unpublished).
[48] A. J. Millis, Phys. Rev. B **48**, 7183 (1993).
[49] A. Ishigaki and T. Moriya, J. Phys. Soc. Jpn. **67**, 3924 (1998).
[50] M. B. Maple, M. C. de Andrade, J. Herrmann, Y. Dalichaouch, D. A. Gajewski, C. L. Seaman, R. Chau, R. Movshovich, M. C. Aronson, and R. Osborn, J. Low Temp. Phys. **99**, 223 (1995).
[51] C. Pfleiderer, D. Reznik, L. Pintschovius, H. von Löhneysen, M. Garst, and A. Rosch, Nature (London) **427**, 227 (2004).
[52] E. Bauer, C. H. Booth, G. H. Kwei, R. Chau, and M. B. Maple, Phys. Rev. B **65**, 245114 (2001).
[53] C. H. Booth, E. W. Scheidt, U. Killer, A. Weber, and S. Kehrein, Phys. Rev. B **66**, 140402 (2002).
[54] I. Maksimov, F. J. Litterst, H. Rechenberg, M. A. C. de Melo, R. Reyerhem, R. W. A. Hendrikx, T. J. Gortenmulder, J. A. Mydosh, and S. Süllow, Phys. Rev. B **67**, 104405 (2003).
[55] Ben-Li Young, D. E. MacLaughlin, M. S. Rose, K. Ishida, O. O. Bernal, H. G. Lukefahr, K. Heuser, G. R. Stewart, N. P. Butch, P.-C. Ho, and M. B. Maple, Phys. Rev. B **70**, 024401 (2004).